

Comparative quantification of numerical mixing estimates from offline budgets of salinity squared and salinity anomaly squared in a coastal ocean model

Dylan Schlichting, Robert Hetland, Lixin Qu, Daijiro Kobashi

The purpose of this document is to derive equations for volume integrated budgets of salinity squared s^2 , salinity anomaly squared s'^2 , and their differences. The goal of deriving these equations is to quantify numerical mixing in the Texas-Louisiana (TXLA) shelf hydrodynamic model, which is based on a realistic implementation of ROMS (Zhang et al., 2012). Both budgets may be used to quantify numerical mixing because numerical advection schemes are not designed to preserve second moments of salinity (i.e. salinity variance), nor is necessary to reference salinity to a volume mean to quantify the associated variance because both budgets contain identical resolved (i.e. physical) mixing. The derivations shown here will have supplementary notes that would otherwise be excluded from a manuscript for both mathematical and conceptual clarification.

1. SALINITY SQUARED BUDGET

Consider a three-dimensional control volume with four open horizontal boundaries. We start with the Reynolds-averaged salinity conservation in Cartesian coordinates that neglects explicit horizontal mixing because the horizontal salinity gradients in the TXLA model are many orders of magnitude smaller than the vertical gradients:

$$\frac{\partial s}{\partial t} + \mathbf{u} \cdot \nabla s = \frac{\partial}{\partial z} \left(K_s \frac{\partial s}{\partial z} \right), \quad (1)$$

where \mathbf{u} is the 3D velocity vector and K_s is the vertical salinity diffusivity. To derive volume integrated budgets of s^2 , and s'^2 , we first consider the local salinity boundary conditions. ROMS parameterizes surface volume fluxes due to evaporation and precipitation as surface salt fluxes, which is to say no water is added or taken away, so the corresponding surface and bottom boundary conditions are:

$$\begin{aligned} -K_s \left(\frac{\partial s}{\partial z} \right) &= -s(E - P) \text{ at } z = \zeta \\ -K_s \left(\frac{\partial s}{\partial z} \right) &= 0 \text{ at } z = -h \end{aligned} \quad (2)$$

where E and P are the evaporation and precipitation per unit area, respectively, ζ is the time-varying free surface, and h is the depth of the ocean bottom below mean sea level. To derive an equation for s^2 and the accompanying boundary conditions, we multiply Equations 1-2 and by 2 s :

$$\frac{\partial s^2}{\partial t} + \mathbf{u} \cdot \nabla s^2 = \frac{\partial}{\partial z} \left(K_s \left(\frac{\partial s^2}{\partial z} \right) \right) - 2K_s \left(\frac{\partial s}{\partial z} \right)^2 \quad (3)$$

$$\begin{aligned} -K_s \left(\frac{\partial s^2}{\partial z} \right) &= -2s^2(E - P) \text{ at } z = \zeta \\ -K_s \left(\frac{\partial s^2}{\partial z} \right) &= 0 \text{ at } z = -h \end{aligned} \quad (4)$$

where $2K_s \left(\frac{\partial s}{\partial z} \right)^2$ is the dissipation of salinity variance that is often denoted as χ or χ^s , which is an unambiguous measure of salinity mixing (Burchard and Rennau, 2008). To form a budget for s^2 , we volume integrate Equations 3-4 over the entire domain:

$$\underbrace{\int_V \frac{\partial s^2}{\partial t} dV}_{\text{Tendency}} + \underbrace{\iint_A (\mathbf{u} s^2) \cdot d\mathbf{A}}_{\text{Boundary advection}} + \underbrace{\iint_{A_{surf}} (-2s^2)(E - P) dA}_{\text{Surface fluxes}} = - \underbrace{\int_V \chi^s dV}_{\text{Resolved mixing}} - \underbrace{M_{num,s^2}}_{\text{Numerical mixing}}, \quad (5)$$

where $d\mathbf{A}$ is the differential area of the lateral control volume boundaries. As shown in Equation 5, there are five terms that affect the evolution of s^2 in a control volume, the volume integrated change of s^2 with respect to time (also denoted as storage in the literature), the advection of s^2 through the lateral boundaries, the addition or removal of s^2 due to evaporation and precipitation, the resolved mixing, and the numerical mixing. It is important to note that the Leibniz rule is not used to pull the time derivative outside of the volume integral in the tendency term because the control volume is assumed to vary with respect to time. Previous studies that have used volume integrated budgets of s^2 and s'^2 to characterize mixing (Burchard et al., 2019; Lorenz et al., 2021; MacCready et al., 2018) often time-average the various terms (i.e. tidal or spring-neap averaging) such that the domain volume is invariant and the time derivative may be pulled outside the volume integral.

The numerical mixing, when calculated offline, is unknown and is subsequently quantified as the residual of Equation 5. In terms of sign convention, both the resolved and numerical mixing are positive definite quantities for monotonic advection schemes, meaning that positive values indicate destruction of variance and negative values indicate creation of variance. Note that Equation 5 is similar to the derivation presented in Burchard et al. (2019), however we include surface fluxes here.

2. SALINITY ANOMALY SQUARED BUDGET

If we define the salinity anomaly squared as $s'^2 = (s - \bar{s})^2$, where \bar{s} is the volume averaged salinity, the salinity anomaly squared equation for the control volume may be obtained by subtracting $\partial_t(\bar{s})$ from Equation 1 and multiplying by $2s'$:

$$\frac{\partial s'^2}{\partial t} + \mathbf{u} \cdot \nabla s'^2 = \frac{\partial}{\partial z} \left(K_s \left(\frac{\partial s'^2}{\partial z} \right) \right) - 2s' \frac{\partial \bar{s}}{\partial t} - 2K_s \left(\frac{\partial s'}{\partial z} \right)^2 \quad (6)$$

We can derive the surface and bottom boundary conditions by multiplying Equation 2 by $2s'$:

$$\begin{aligned} -K_s \left(\frac{\partial s'^2}{\partial z} \right) &= -2(E - P)s^2 + 2(E - P)s\bar{s} \text{ at } z = \zeta \\ -K_s \left(\frac{\partial s'^2}{\partial z} \right) &= 0 \text{ at } z = -h \end{aligned} \quad (7)$$

To form the salinity anomaly squared budget, we volume integrate Equations 6-7:

$$\underbrace{\int_V \frac{\partial s'^2}{\partial t} dV}_{\text{Tendency}} + \underbrace{\iint_A (\mathbf{u} s'^2) \cdot d\mathbf{A}}_{\text{Boundary advection}} + \underbrace{\iint_{A_{surf}} (-2s^2 + 2s\bar{s})(E - P) dA}_{\text{Surface fluxes}} = \underbrace{-2 \int_V K_s \left(\frac{\partial s'}{\partial z} \right)^2 dV}_{\text{Resolved mixing}} - \underbrace{M_{num,s'^2}}_{\text{Numerical mixing}} \quad (8)$$

Similar to the s^2 budget, the s'^2 is controlled by five terms: tendency, lateral boundary advection, fluxes of variance through the vertical control surface, resolved mixing, and numerical mixing. It should be noted that the resolved mixing is the same for both budgets because the the vertical gradient of the salinity anomaly s' may be written as $\frac{\partial(s-\bar{s})}{\partial z}$ and \bar{s} has no spatial gradients, therefore the two are equivalent.

Anticipating expressing s in terms of $\bar{s} + s'$ in the following section, we rewrite the surface flux term as follows:

$$\begin{aligned} \iint_{A_{surf}} K_s \frac{\partial s'^2}{\partial z} dA &= \iint_{A_{surf}} [-2(\bar{s} + s')^2 + 2\bar{s}(\bar{s} + s')] (E - P) dA \\ &= \iint_{A_{surf}} (-2\bar{s}^2 - 4\bar{s}s' - 2s'^2 + 2\bar{s}^2 + 2\bar{s}s') (E - P) dA \\ &= \iint_{A_{surf}} (-2\bar{s}s' - 2s'^2) (E - P) dA \end{aligned} \quad (9)$$

3. DIFFERENCES BETWEEN s^2 AND s'^2 BUDGETS

To demonstrate the differences between the s^2 and s'^2 budgets, we use a Reynolds decomposition to express the s equation in terms of \bar{s} and s' :

$$\frac{\partial(\bar{s} + s')}{\partial t} + \mathbf{u} \cdot \nabla(\bar{s} + s') = \frac{\partial}{\partial z} \left(K_s \left(\frac{\partial(\bar{s} + s')}{\partial z} \right) \right) \quad (10)$$

If we note that \bar{s} has no spatial gradients and multiply Equation 10 by $2(\bar{s} + s')$, we arrive at the s^2 Equation in terms of \bar{s} and s' :

$$(2\bar{s} + 2s') \left(\frac{\partial \bar{s}}{\partial t} + \frac{\partial s'}{\partial t} \right) + (2\bar{s} + 2s') [\mathbf{u} \cdot \nabla(\bar{s} + s')] = (2\bar{s} + 2s') \left[\frac{\partial}{\partial z} \left(K_s \left(\frac{\partial \bar{s}}{\partial z} + \frac{\partial s'}{\partial z} \right) \right) \right] \quad (11)$$

Expanding, we have:

$$\begin{aligned} \frac{\partial \bar{s}^2}{\partial t} + 2\bar{s} \frac{\partial s'}{\partial t} + 2s' \frac{\partial \bar{s}}{\partial t} + \frac{\partial s'^2}{\partial t} + \mathbf{u} \cdot \nabla(\bar{s}^2 + 2\bar{s}s' + s'^2) = \\ \frac{\partial}{\partial z} \left(K_s \left(\frac{\partial \bar{s}^2}{\partial z} + \frac{\partial s'^2}{\partial z} \right) \right) - 2K_s \left(\frac{\partial \bar{s}}{\partial z} + \frac{\partial s'}{\partial z} \right)^2 \end{aligned} \quad (12)$$

We apply a similar decomposition to the surface salinity boundary conditions and multiply by $2(\bar{s} + s')$:

$$\begin{aligned} (2\bar{s} + 2s') \left[-K_s \left(\frac{\partial \bar{s}}{\partial z} + \frac{\partial s'}{\partial z} \right) \right] = -(2\bar{s} + 2s')(\bar{s} + s')(E - P) \text{ at } z = \zeta \\ (2\bar{s} + 2s') \left[-K_s \left(\frac{\partial \bar{s}}{\partial z} + \frac{\partial s'}{\partial z} \right) \right] = 0 \text{ at } z = -h \end{aligned} \quad (13)$$

Expanding and simplifying:

$$\begin{aligned} -K_s \left(\frac{\partial \bar{s}^2}{\partial z} + 2\bar{s} \frac{\partial s'}{\partial z} + 2s' \frac{\partial \bar{s}}{\partial z} + \frac{\partial s'^2}{\partial z} \right) = (-2\bar{s}^2 - 4\bar{s}s' - 2s'^2)(E - P) \text{ at } z = \zeta \\ -K_s \left(\frac{\partial \bar{s}^2}{\partial z} + 2\bar{s} \frac{\partial s'}{\partial z} + 2s' \frac{\partial \bar{s}}{\partial z} + \frac{\partial s'^2}{\partial z} \right) = 0 \text{ at } z = -h \end{aligned} \quad (14)$$

Volume integrating, noting that the volume integral of s' is zero and \bar{s} has no spatial gradients, we have:

$$\begin{aligned} & \underbrace{\frac{d\bar{s}^2}{dt} V + 2\bar{s} \int_V \frac{\partial s'}{\partial t} dV}_{\text{Extra tendency}} + \underbrace{\int_V \frac{\partial s'^2}{\partial t} dV}_{\text{Same tendency}} + \underbrace{\int \int_A \mathbf{u} \cdot d\mathbf{A}}_{\text{Extra advection}} + \underbrace{\int \int_A (\mathbf{u}s') \cdot d\mathbf{A}}_{\text{Same advection}} + \underbrace{\int \int_A (\mathbf{u}s'^2) \cdot d\mathbf{A}}_{\text{Same advection}} \\ & + \underbrace{\int \int_A (-2\bar{s}^2 - 2\bar{s}s')(E - P) dA}_{\text{Extra surface fluxes}} + \underbrace{\int \int_A (-2\bar{s}s' - 2s'^2)(E - P) dA}_{\text{Same surface fluxes}} = \underbrace{- \int_V \chi^s dV}_{\text{Same resolved mixing}} - \underbrace{M_{num,s^2}}_{\text{Same numerical mixing}} \end{aligned} \quad (15)$$

As shown in Equation 15, there are five extra terms that appear when expressing s^2 in terms of s'^2 , a tendency term, two advection terms, and a surface flux term. To formally quantify differences in numerical mixing estimates between the s^2 and s'^2 budgets, we subtract Equation 15 from Equation 8:

$$\frac{d\bar{s}^2}{dt} V + 2\bar{s} \int_V \frac{\partial s'}{\partial t} dV + \bar{s}^2 \int \int_A \mathbf{u} \cdot d\mathbf{A} + 2\bar{s} \int \int_A (\mathbf{u}s') \cdot d\mathbf{A} + \int \int_A (-2\bar{s}^2 - 2\bar{s}s')(E - P) dA = -M_{num,s^2} + M_{num,s'^2}. \quad (16)$$

4. EXAMPLE APPLICATION: IDEALIZED SHELF MODEL (SHELFSTRAT)

As a simple test case, we examine the differences between the s^2 and s'^2 , budgets in a subset of an idealized continental shelf model (shelfstrat) developed by Hetland (2017). The model is a realistic implementation of ROMS and is configured as a reentrant channel with uniformly sloping bathymetry with added noise to induce instability formation. The model grid is 256 X 128 grid points with a 1 km uniform

horizontal resolution and 30 vertical layers concentrated near the surface and bottom boundary layers. The model is run as an unforced initial value problem no surface fluxes and the initial tracer field designed to be similar to observations of the Mississippi–Atchafalaya plume. There is a constant cross-shore density gradient determined exclusively by salinity inshore of 50 m depth and the horizontally uniform vertical stratification is determined by temperature. The initial flow field is configured with a geostrophic vertical shear with a no slip boundary condition at the seafloor.

Here, we use a modified version of the base case described in Hetland (2017). We ran the model for 30 days, outputting the average and diagnostic files every 30 minutes resulting in 1440 time points. The control volume used for the analysis is displayed in Figure 1 and the accompanying budgets were analyzed from $t = 1300 - 1400$. The accompanying s^2 and s'^2 budgets are shown in Figures 2-3. For both budgets, the numerical mixing is small relative to the other terms, however it is evident that the dynamics of both budgets are different. The s^2 budget is dominated by the tendency and advection terms, with both mixing terms being secondary. On the other hand, the s'^2 budget is dominated by the resolved vertical mixing as well as the tendency term. For the period analyzed here, the resolved mixing is nearly steady state. It is also worth noting that the advection and storage terms of the s^2 budget are approximately one order of magnitude larger than in the s'^2 budget, which makes intuitive sense because the s'^2 budget removes the effect of the mean salinity.

The numerical mixing is much larger and more unsteady in the s^2 budget compared to the s'^2 budget. Without an online calculation of the numerical mixing, it is difficult to confirm which budget provides the *true* estimate of the spurious advection scheme created by the advection scheme. Figure 4 shows that the differences in numerical mixing between the two budgets may be quantified by subtracting the volume integrated s^2 equation from the s'^2 equation to nearly machine precision. The residual here is 10^{-9} , however it is worth noting that model output variables were only outputted to single precision and double precision would further improve the accuracy.

To confirm that the extra terms in Equation 16 are correct, Figures 5-6 examine the extra tendency and advection terms separately. The addition of the extra tendency terms and the difference of the s^2 and s'^2 tendency terms have a residual of 10^{-8} , validating Equation 16. As shown in Figure 6, the addition of the s^2 and s'^2 advection terms have a residual of $10 \text{ m}^3 \text{ s}^{-1} (\text{g kg}^{-1})^2$, however sensitivity experiments show that this is caused by precision errors when pulling \bar{s} outside of the area of the integral. However, this small residual is negligible because the extra advection terms are of order 10^5 , resulting in a relative error of $10/10^5 \approx .01\%$. This may be alleviated by outputting the model variables to double precision and will become increasingly smaller the larger the control volume size becomes.

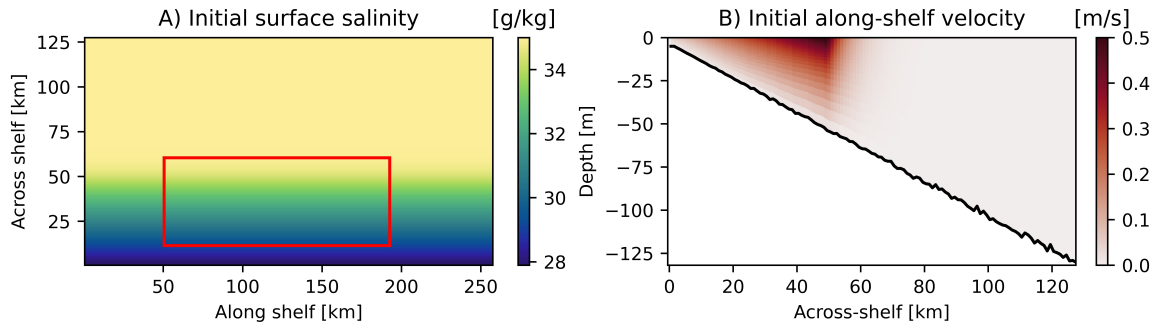


Figure 1: Overview of shelfstrat initial conditions, displaying the A) Initial surface salinity field with the control volume used for the budget analysis in red, and B) Sample cross section of the initial along-shelf velocity.

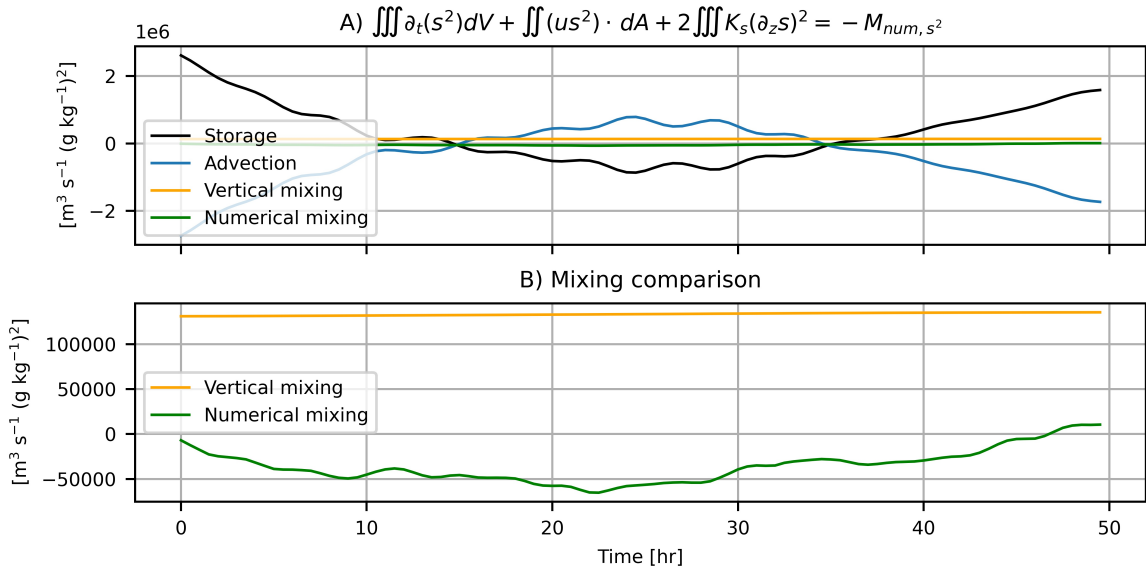


Figure 2: A) Terms in the s^2 budget, and B) comparison between the resolved and numerical mixing.

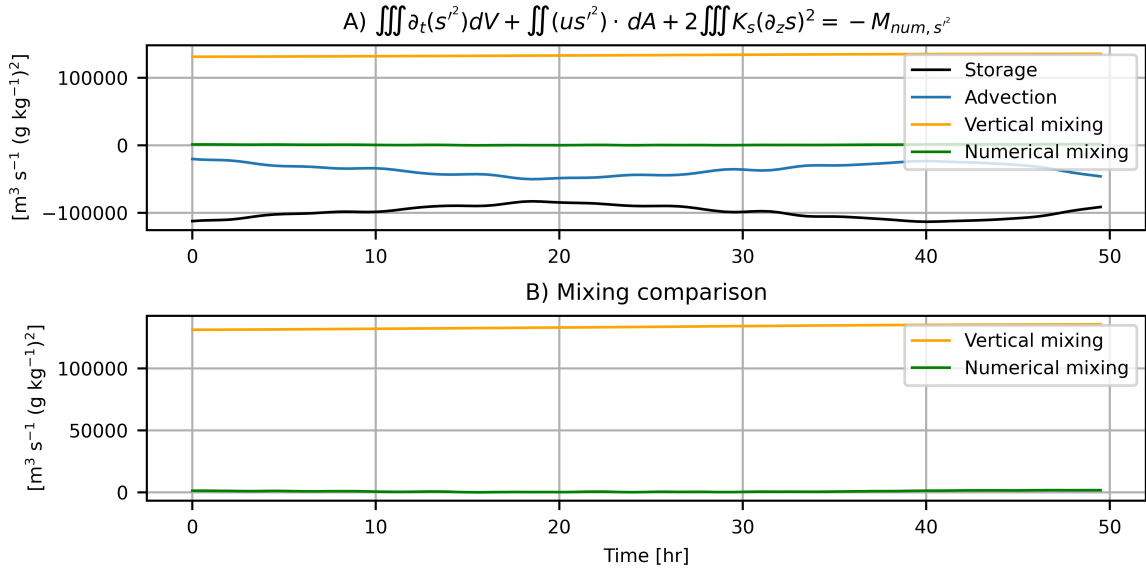


Figure 3: A) Terms in the s'^2 budget, and B) Comparison between the resolved and numerical mixing.

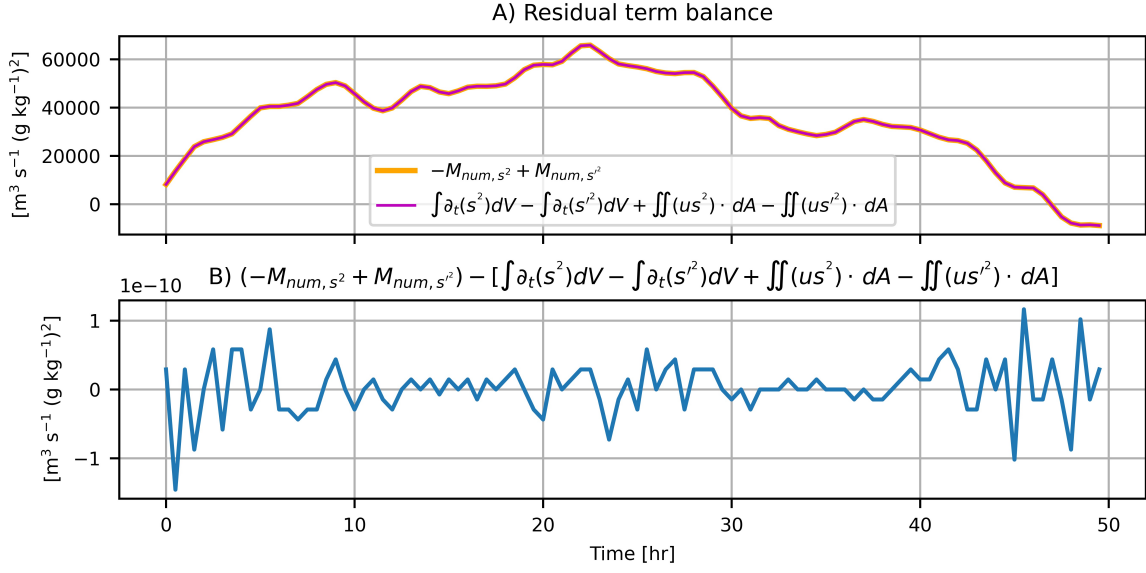


Figure 4: A) Term balance elucidating the results of Equation 16 and B) Residual of Equation 16.

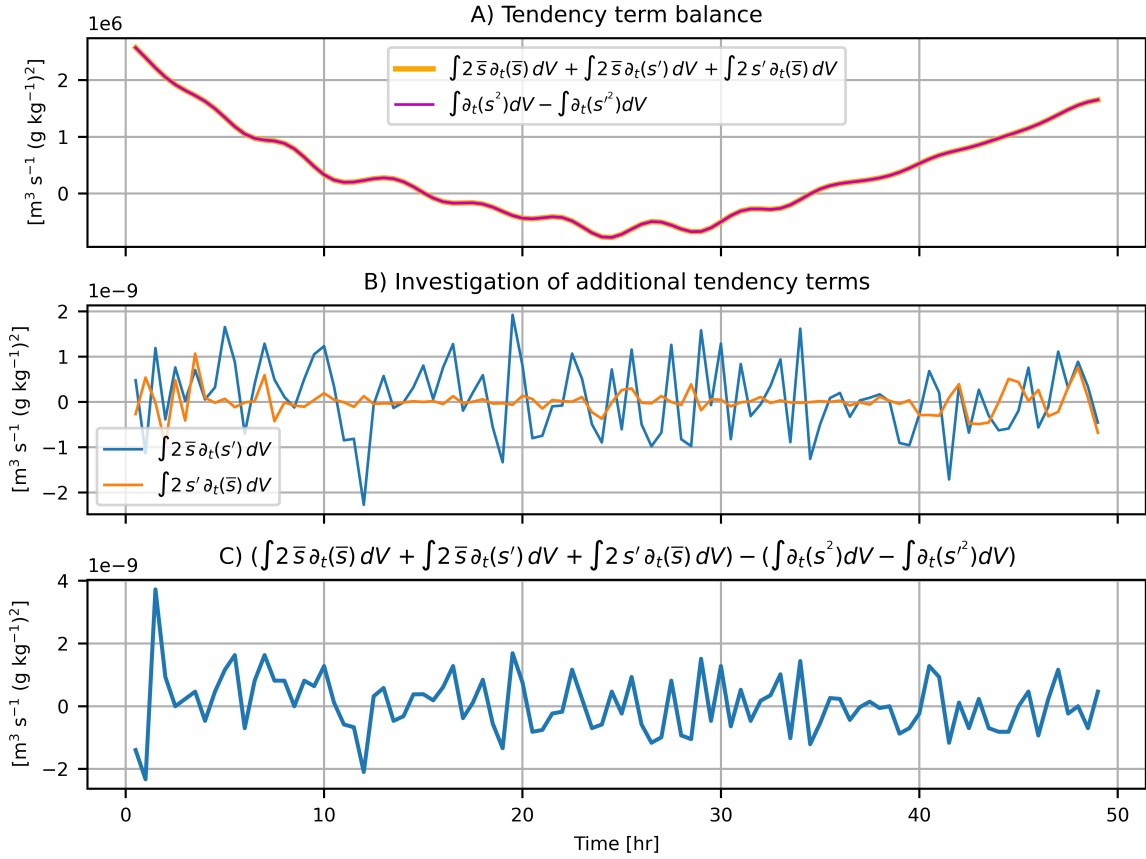


Figure 5: A) Comparison of the extra tendency terms of Equation 15 and the difference between the s^2 and s'^2 tendency terms. B) Proof that $\int_V 2s \partial_t(s') dV$ and $\int_V 2s' \partial_t(\bar{s}) dV$ go to zero and may be excluded from the Equation 15. C) Residual of the extra tendency terms and difference between the s^2 and s'^2 tendency terms.

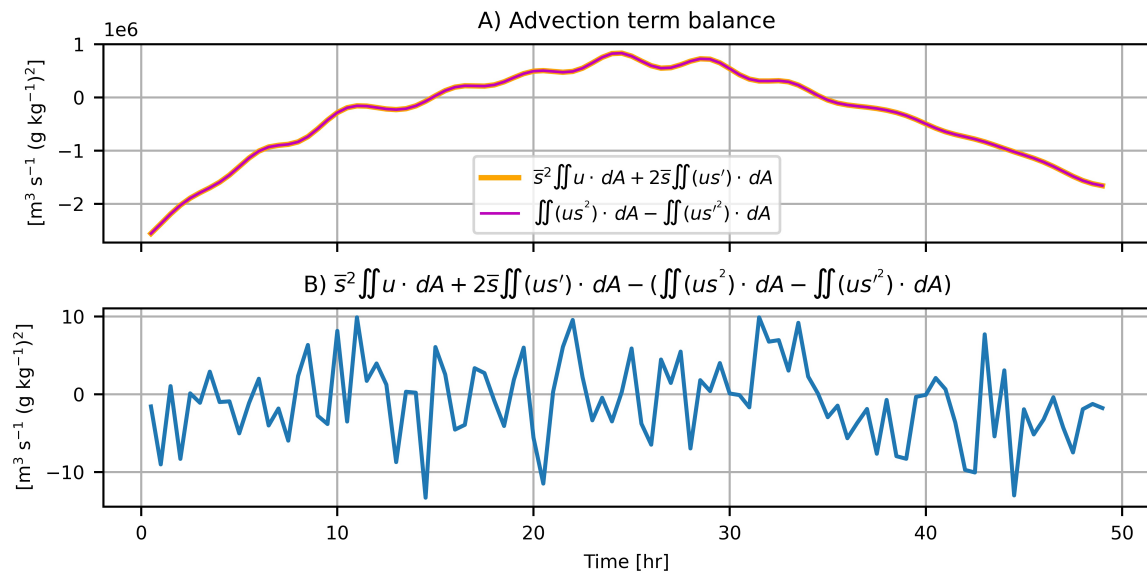


Figure 6: A) Comparison of the extra advection terms of Equation 15 and the difference between the s^2 and s'^2 advection terms. B) Residual of the difference between the extra advection terms and the s^2 and s'^2 advection terms.

5. APPENDIX - SUPPLEMENTAL DERIVATION NOTES

a. Use of the product rule to derive s^2 and s'^2 equations

When multiplying the salt equation by $2s$ to derive the s^2 equation, two versions of the product rule are used. The product rule states that $d(uv) = u(dv) + v(du)$, where u and v are arbitrary functions. To apply this to the s^2 derivation, take the tendency term and let $u = v = s$:

$$\frac{\partial s^2}{\partial t} = \frac{\partial(ss)}{\partial t} = s \frac{\partial s}{\partial t} + s \frac{\partial s}{\partial t} = 2s \frac{\partial s}{\partial t}, \quad (17)$$

which elucidates how multiplying the s equation by $2s$ yields s^2 values on the LHS. Applying the product rule again to the RHS of the s^2 derivation, we have:

$$(2s) \frac{\partial}{\partial z} \left(K_s \frac{\partial s}{\partial z} \right) \rightarrow \frac{\partial}{\partial z} \left((2s) \left(K_s \frac{\partial s}{\partial z} \right) \right), \quad (18)$$

where $u = 2s$, $v = K_s \frac{\partial s}{\partial z}$, and $d(uv) = \frac{\partial}{\partial z}(2s(K_s \frac{\partial s}{\partial z}))$. The product rule may be rearranged such that $u(dv) = d(uv) - v(du)$, leading the RHS of the s^2 equation:

$$\frac{\partial}{\partial z} \left((2s) \left(K_s \frac{\partial s}{\partial z} \right) \right) - K_s \left(\frac{\partial s}{\partial z} \left(\frac{\partial}{\partial z}(2s) \right) \right) \quad (19)$$

$$= \frac{\partial}{\partial z} \left(K_s \left(\frac{\partial s^2}{\partial z} \right) \right) - 2K_s \left(\frac{\partial s}{\partial z} \right)^2 \quad (20)$$

b. Proof that $\int_V s' dV = 0$

Let $s = \bar{s} + s'$ where $\bar{s} = (1/V) \int_V s dV$ as in Section 2. It follows that:

$$\int_V s dV = \int_V \bar{s} dV + \int_V s' dV. \quad (21)$$

Substituting $\bar{s} = s - s'$, we have:

$$\begin{aligned} \int_V s dV &= \int_V (s - s') dV + \int_V s' dV \\ \int_V s dV &= \int_V s dV - \int_V s' dV + \int_V s' dV \\ \int_V s dV &= \int_V s dV \rightarrow \therefore \int_V s' dV = 0 \end{aligned} \quad (22)$$

REFERENCES

- Burchard, H., Lange, X., Klingbeil, K., and MacCready, P. (2019). Mixing estimates for estuaries. *Journal of Physical Oceanography*, 49(2):631–648.
- Burchard, H. and Rennau, H. (2008). Comparative quantification of physically and numerically induced mixing in ocean models. *Ocean Modelling*, 20(3):293–311.
- Hetland, R. D. (2017). Suppression of baroclinic instabilities in buoyancy-driven flow over sloping bathymetry. *Journal of Physical Oceanography*, 47(1):49–68.
- Lorenz, M., Klingbeil, K., and Burchard, H. (2021). Impact of evaporation and precipitation on estuarine mixing. *Journal of Physical Oceanography*, 51(4):1319–1333.
- MacCready, P., Geyer, W. R., and Burchard, H. (2018). Estuarine exchange flow is related to mixing through the salinity variance budget. *Journal of Physical Oceanography*, 48(6):1375–1384.
- Zhang, X., Marta-Almeida, M., and Hetland, R. (2012). A high-resolution pre-operational forecast model of circulation on the Texas-Louisiana continental shelf and slope. *Journal of Operational Oceanography*, 5(1):19–34.